

# VISUAL REALISM ASSESSMENT FOR FACE-SWAP VIDEOS

Xianyun Sun<sup>1,+</sup>, Beibei Dong<sup>2</sup>, Caiyong Wang<sup>1</sup>, Bo Peng<sup>2,\*</sup>, Jing Dong<sup>2</sup>

## ABSTRACT

Deep-learning based face-swap videos, also known as deep-fakes, are becoming more and more realistic and deceiving. The malicious usage of these face-swap videos has caused wide concerns. The research community has been focusing on the automatic detection of these fake videos, but the assessment of their visual realism, as perceived by human eyes, is still an unexplored dimension. Visual realism assessment, or VRA, is essential for assessing the potential impact that may be brought by a specific face-swap video, and it is also important as a quality assessment metric to compare different face-swap methods. In this paper, we make a small step towards this new VRA direction by building a benchmark for evaluating the effectiveness of different automatic VRA models, which range from using traditional hand-crafted features to different kinds of deep-learning features. The evaluations are based on a recent competition dataset named as DFGC-2022, which contains 1400 diverse face-swap videos that are annotated with Mean Opinion Scores (MOS) on visual realism. Comprehensive experiment results using 11 models and 3 protocols are shown and discussed. We demonstrate the feasibility of devising effective VRA models for assessing face-swap videos and methods. The particular usefulness of existing deepfake detection features for VRA is also noted. *The code and benchmark will be made publicly available.*

**Index Terms**— Deepfake, Face-swap, Realism Assessment, benchmark

## 1. INTRODUCTION

Face-swap videos, as the name indicates, are videos in which the appearance of a face is manipulated using computer programs (especially deep learning based methods) so that audiences may recognize the face as another individual. This technology has contributed a lot to filming and other entertainment industry, yet holding a high risk of being abused.

<sup>+</sup> The work was done while Xianyun Sun was an intern at CASIA.

<sup>\*</sup> Bo Peng is the corresponding author.

<sup>1</sup> School of Electrical and Information Engineering, Beijing University of Civil Engineering and Architecture, Beijing 100044, China (e-mail: sunxianyun@stu.bucea.edu.cn, wangcayong@bucea.edu.cn)

<sup>2</sup> State Key Laboratory of Multimodal Artificial Intelligence Systems (MAIS), Institute of Automation, Chinese Academy of Sciences (CASIA), Beijing 100190, China (e-mail: dongbeibei2022@ia.ac.cn, bo.peng@nlpr.ia.ac.cn, jdong@nlpr.ia.ac.cn)

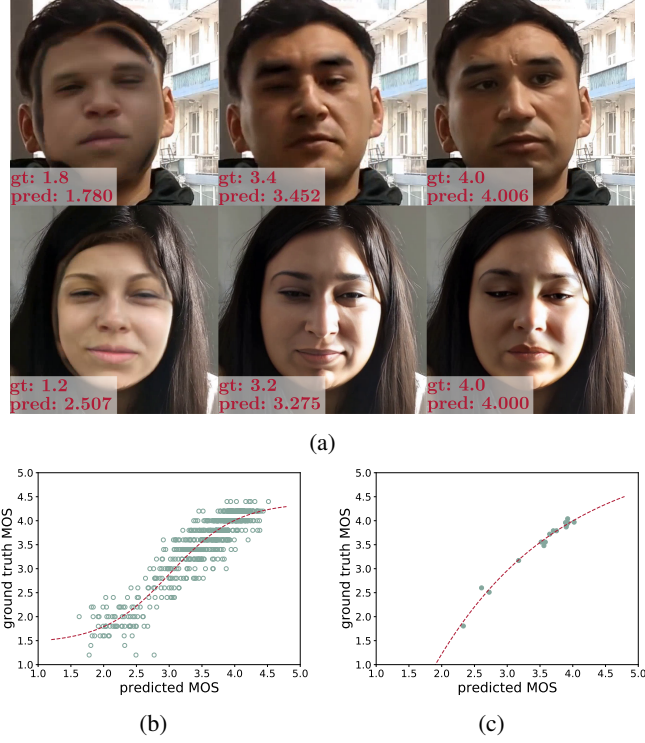


**Fig. 1:** (a) Face-swap videos with different degrees of realism, annotated with the ground truth MOS (*gt*) vs predicted MOS (*pred*) by the DFGC-1st VRA model. (b) and (c) are scatter plots with the fitted logistic curves (see Subsection 4.1). (b) is the video-level plot and (c) is the method-level plot.

The detection methods against face-swap videos, or deep-fakes, have improved a lot with intense attentions being drawn [1]. Since the ultimate goal of face-swapping is to serve human viewers, subjective realism assessment could play a critical role not only in estimating the influence of fake videos on social networks, but also in evaluating the performance of face-swapping models during their development.

Several studies have been carried out to explore the subjective opinions on the persuasiveness of deepfake media. Deep models such as MOSNet [2] and MOSA-Net [3] are developed for assessing the naturalness of converted speeches. Compared with deepfake audios, relatively fewer studies have been carried out on deepfake images or videos. Nightingale

et al. [4, 5] conduct subjective evaluations on StyleGAN2 generated images and find that the synthetic faces are indistinguishable from and even more trustworthy than real faces. Korshunov and Marcel [6] conduct a subjective study on face-swap videos from the DFDC dataset and find that human perception is very different from the machine perception, and they are both successfully but in different ways fooled by deepfakes. All these studies, however, only demonstrate human’s performance in deepfake detection, with none of them providing any method to estimate the realism degree of deepfakes. A model proposed in [7] is trained to predict subjective quality for GAN-generated facial images, which is the only model of its kind to the best of our knowledge. There is an obvious vacant position for models assessing the visual realism of deepfake videos.

Here in this paper, we build the first visual realism assessment (VRA) benchmark for face-swap videos as an attempt to fill this gap. In our proposed method, models from related fields are employed as feature extractors, with support vector regression (SVR) as the regressor mapping features to a predicted subjective realism score. Fig. 1a shows a demo of some fake videos’ frames with the groundtruth mean opinion score (MOS) and predicted MOS. Fig. 1b and Fig. 1c show a general view of the correlation between the prediction and the groundtruth on the DFGC-2022 dataset, in video-level and method-level (i.e. face-swap methods assessed) respectively.

In the following parts, Section 2 gives a brief overview of the DFGC-2022 dataset, on which our work is based. Section 3 introduces the proposed VRA method. Experiment details and results are discussed in Section 4, and Section 5 summarizes this work.

## 2. DATASET ANALYSIS

Originated from the Second DeepFake Game Competition (DFGC) [8] held with the IJCB-2022 conference, the DFGC-2022 dataset contains a total of 2799 face-swap videos and 1595 real videos, all about 5s in length. Fake clips in the dataset are generated by various face-swap methods (e.g. DeepFaceLab [9], SimSwap [10], FaceShifter [11]) and post-processing operations, and they are submitted by the participants through three separate submission sessions, i.e., C1, C2, and C3. This forms three subsets, with their details shown in Table 1. Each submission is associated with a submit-id and contains 80 swap videos for 20 pairs of facial-IDs. The fake clips from the same submit-id are deemed to be created by

**Table 1:** Details of C1, C2, and C3 subset in DFGC-2022

subset	annotated fake clips	facial-ids	submit-ids
C1	240	20 pairs	6
C2	520	20 pairs	13
C3	640	20 pairs	16

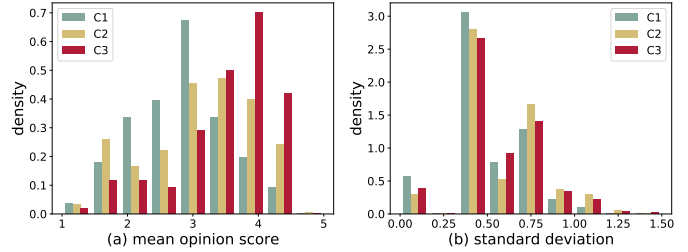


**Fig. 2:** Histograms of the mean and standard deviation of each video’s realism rating in DFGC-2022.

the same method or process. 40 clips in each submission are annotated by 5 human raters independently in the aspect of video realism, apart from some other aspects. The rating is from 1 (very bad) to 5 (very good). The mean opinion score (MOS) and the standard deviation of each video’s ratings are calculated and their distributions are shown in Fig. 2.

## 3. VRA METHODS

In this section, we will go through the workflow of the VRA methods. First, we crop the face area from each frame in the data pre-processing step. Then, per-frame features are extracted using existing hand-crafted or deep-learning models. And finally, the per-frame features are fused into the video-level feature, which goes through a feature selection step before it is used to regress the video realism score. Here we follow the classical video quality assessment workflow [12] to construct our own, which is in contrast to learning end-to-end deep models for VRA, e.g. using LSTM and GRU models. This is because deep models heavily rely on the amount of training data, which is not suitable in our case, considering that there are only several hundreds of annotated training videos in the DFGC-2022 dataset.

### 3.1. Data Pre-processing

The videos in DFGC-2022 dataset have the resolution of  $1080 \times 1920$ , with the speaker’s face taking over less than 25% of the area. Since VRA for face-swap should focus more on the facial area than the backgrounds, we crop each video according to detected face bounding boxes. For the fairness of comparing different face-swap methods, the face detection is only performed on the original target videos, and the result boxes are shared by all face-swap videos that originate from the same target video.

Specifically, we first enlarge the detected boxes by 1.3 times to include the full head region. We then obtain the smallest box that encapsulate all face boxes in the video and use it to crop all the video frames. This cropping strategy prevents the jittering of consecutive cropped frames. Cropped videos shrunk to about  $600 \times 600$ , which is also beneficial for the time efficiency of following processes. Table 2 shows that

conducting VRA on facial crops greatly improves prediction accuracy and efficiency than directly using full-frames.

**Table 2:** Comparison of efficiency and prediction accuracy without and with cropping, using the VIDEVAL model.

Cropping	Time↓	PLCC↑	RMSE↓
w/o	69.04s	0.5687	0.5806
w/	25.49s	0.7715	0.4552

### 3.2. Feature Extraction

When selecting feature extractors, we employ several representative models from the subjective image/video quality assessment, image recognition, face recognition, and deepfake detection fields, with the consideration of potential feature sharing between VRA and these tasks. Table 3 summarises the models included in our evaluation. IQA and VQA respectively refers to Image Quality Assessment and Video Qualtiy Assessment. The *original* part in the *feats dim* column refers to the dimension of the original video-level features extracted by each model, and the *selected* part denotes the dimension after our feature selection step.

**Table 3:** Overview of the feature extraction models.

Model	Original Task	feats dim		Training Data
		original	selected	
BRISQUE	IQA	72	72	hand-crafted
GM-LOG	IQA	80	80	hand-crafted
FRIQUEE	IQA	1120	1120	hand-crafted
TLVQM	VQA	75	75	hand-crafted
V-BLIINDS	VQA	46	46	hand-crafted
VIDEVAL	VQA	60	60	hand-crafted
ensemble	VQA	3229	240	hand-crafted
ResNet50	image recognition	4096	160	ImageNet
VGG-Face	face recognition	8192	280	VGG-Face
DFDC-ispl	deepfake detection	3584	100	FF++, DFDC
DFGC-1st	deepfake detection	11264	260	9 deepfake datasets

**IQA Features.** Natural scene statistics (NSS) models assume that natural image pixels follow a generalized Gaussian distribution (GGD) after passing a band-pass filter, with the GGD shape and variance related only to the image quality. Many IQA models are based on the NSS model with different choices of band-pass filters. Statistics are then calculated based on the filtered images to form the IQA features.

BRISQUE [13] is a typical IQA model under the NSS framework, adopting mean subtracted contrast normalized (MSCN) coefficients as its band-pass filter. The FRIQUEE model [14] further extends the application of NSS model from gray scale to multiple color spaces including RGB, LAB and LMS. GM-LOG [15] uses isotropic differential operators in replacement of band-pass transforms, including the Gradient Magnitude (GM) and Laplacian of Gaussian (LOG) operators.

**VQA Features.** Different from IQA features that only focus on single frames, VQA features also represent the tem-

poral information. TL-VQM [16] includes statistical features of the motion vectors between every two consecutive frames. None NSS-based frame features are also designed for detecting dark or bright areas, blockiness, sharpness, noises and other distortion. V-BLIINDS [17] also includes features of the motion vectors and includes DCT features extracted from frame differences.

VIDEVAL [12] packs up features from BRISQUE [13], GMLOG [15], FRIQUEE [14] and TLVQM [16] and employs an additional feature selection process. With a reduced feature dimension of only 60, VIDEVAL is able to achieve SOTA performances for the VQA task using hand-craft features. Inspired by VIDEVAL, we propose a new “ensemble” model that extends VIDEVAL’s feature candidates to also include features from V-BLIINDS [17] and the hand-craft features in RAPIQUE [18]. Similarly, the feature selection process is conducted, as will be introduced in Section 3.3.

**General Image Recognition Features.** In existing VQA literature, it has been shown that features extracted by general-purpose image recognition models like VGG [19] and ResNet [20] pre-trained on ImageNet can be potential video quality indicators with an additional regressor on top. This makes it a natural choice for us to also include the image recognition features in our evaluation. A ResNet-50 pre-trained on the ImageNet database is adopted, and we resize the images according to its input requirements.

**Face Recognition Features.** VGG-Face [21] is selected as the representative face recognition model for feature extraction. It achieves a remarkable face recognition accuracy using a VGG-19 model finetuned on the VGG-Face dataset including 2622 identities. We select it as the representative face recognition model for its simplicity and high performance, although other advanced face recognition models can also be considered.

**Deepfake Detection Features.** Since our VRA benchmark is based on the DFGC-2022 dataset, the 1st-place solution [22] in DFGC-2022 detection track (referred to as DFGC-1st) is a natural candidate for evaluation. Two ConvNext at different epochs and a Swin-Transformer are employed in this solution, and they are trained on an abundant collection of 9 deepfake datasets with data augmentation and two-class classification loss. Note that the DFGC-2022 dataset itself is not in the training data of this model.

As a comparison, we also include a top 2% solution [23] from the ISPL team in the DFDC challenge [23] (referred to as DFDC-ispl). This solution employs a single EfficientNet with extra attention blocks, which is trained on two datasets, i.e., FaceForensics++ and DFDC.

### 3.3. Realism Score Regression

**Video-level Feature Fusion.** Apart from the VQA features, i.e., TLVQM, V-BLIINDS, VIDEVAL and ensemble, that are already extracted as video-level features following

their original fusion designs, the rest are per-frame features and need to be fused to video-level features. With frame features  $f_1, f_2, \dots, f_n$  extracted from  $n$  sampled frames, average pooling ( $f_{mean}$ ) and standard deviation pooling ( $f_{std}$ ) are the two most popular feature aggregation methods in the VQA field, which are also adopted in our work. They are expressed as:

$$f_{mean} = \frac{1}{n} \sum_{i=1}^n f_i \quad (1)$$

$$f_{std} = \frac{1}{n-1} \sum_{i=1}^n \sqrt{(f_i - f_{ave})^2} \quad (2)$$

Note that  $f_{mean}$  and  $f_{std}$  each has the same feature dimension as the frame features, and they are concatenated to form the video-level features. Take the ResNet50 model in Table 3 as example, the dimension of frame features extracted by the model is 2048, then the fused video-level feature dimension becomes 4096 after concatenating the mean and std.

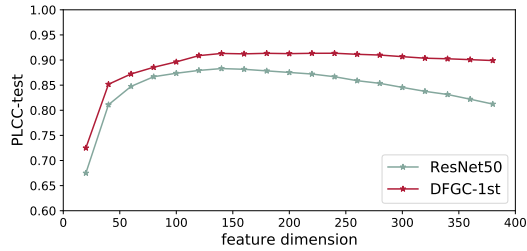


**Fig. 3:** PLCC under different selected feature dimensions.

**Feature Selection.** The performance and efficiency of our regressor, which is a SVR here, drop prominently when feature dimension grows too large, indicating a need for feature selection. Fig. 3 shows how the accuracy of ResNet50 and DFGC-1st changes with the dimension of selected features. Our feature selections are conducted for the ensemble, ResNet50, VGG-Face, DFDC-ispl, and DFGC-1st models, as their original feature dimensions are relatively high, as shown in Table 3.

Following the VQA work presented in [12], we implement a similar two-stage feature selection strategy. In both selection stages, feature importance is ranked by a SVR with the linear kernel. In the first stage, the optimal number of features  $k$  is selected by grid-search over the range of total feature dimensions in a step of 20. The  $k$  giving the best average PLCC in 10 random train-test iterations is chosen. Each feature extraction model has its own optimal  $k$ , as shown in the *selected* sub-column of Fig. 3. In the second stage, 100 iterations are performed with the optimal  $k$ , resulting in 100 subsets of chosen features. The frequency of each feature being selected over these iterations is recorded, and the top- $k$  most frequent features are selected as the final selected features. More details can be found in [12].

**Score Regression.** With each model’s selected features as the input, support vector regression (SVR) models are trained to regress the groundtruth MOS of video realism, using L2 loss. For this score regression step, we use the SVR model with RBF kernel, and set its hyper-parameters  $C$  and  $\gamma$  by grid-search using a random 20% of the training data as the validation set. Finally, the regressor is trained again on the whole training set with the searched hyper-parameters.

## 4. EXPERIMENT RESULTS

### 4.1. Evaluation Protocols and Metrics

Since C3 is the session with the largest number of submissions, as shown in Table 1, we train our models exclusively on the C3 subset of DFGC-2022. We report both intra-subset and inter-subset performances, where the former trains on a portion of C3 videos and tests on the rest C3 videos, while the latter trains on C3 and tests on C1, C2, and even real videos.

For the intra-subset evaluation, we report model performances using three different protocols: the *video level facial-id* split, the *video level submit-id* split, and the *method level submit-id* split. In the facial-id split, 4 out of 20 ID pairs (128 out of 640 videos) are chosen as the test set, and the rest are the train set. In the submit-id splits, 3 out of 16 submit-IDs (120 out of 640 videos) are chosen as the test set. To reduce the impact of randomness, 100 train-test iterations are performed with different choices of facial-ids or submit-ids across iterations. A random seed equals to the iteration number is set to ensure the uniformity of splits when testing different models. Different from the video level protocols that calculate prediction accuracy for videos, the method level protocol aims to evaluate the overall quality of different face-swap methods with respect to the realism of their created videos. For method level evaluation, the groundtruth method MOS is calculated by the average of groundtruth MOS of videos in the same submit-id, and the predicted method MOS is the average of predicted MOS of these videos.

For the inter-subset evaluations, the models are trained on all C3 videos and tested on all C1 or C2 videos, or tested on 120 corresponding real target videos in the three sessions. It is a more challenging protocol that can reflect the generalization ability of evaluated models. This is because C2 and C1 videos are created by different face-swap methods from C3 and their MOS has different distributions, as shown in Fig. 2. And real videos are not seen during training, which should have groundtruth MOS of 5 (best realism). Note that, in the inter-subset setting, the selected features and hyper-parameters are all the same from those in the intra-subset setting, meaning that the models are not fine-tuned from sets to sets.

Following the VQA literature, SRCC (Spearman rank-order correlation coefficient), PLCC (Pearson linear correlation coefficient) and RMSE (root mean square error) are employed as evaluation metrics in our benchmark. The

**Table 4:** Performance comparison of VRA models.

Metric	SRCC↑(std)			PLCC↑(std)			RMSE↓(std)		
	facial-id (video)	submit-id (video)	submit-id (method)	facial-id (video)	submit-id (video)	submit-id (method)	facial-id (video)	submit-id (video)	submit-id (method)
<b>BRISQUE</b>	0.2646(.104)	0.5379(.202)	0.6906(.453)	0.4185(.124)	0.5803(.198)	0.7687(.453)	0.6473(.055)	0.4208(.135)	0.2730(.226)
<b>GM-LOG</b>	0.4324(.097)	0.5160(.229)	0.6970(.476)	0.5630(.088)	0.5657(.226)	0.7500(.472)	0.5907(.053)	0.4152(.114)	0.2887(.209)
<b>FRIQUEE</b>	0.5281(.084)	0.6481(.165)	0.8120(.347)	0.6926(.078)	0.6928(.175)	0.8712(.312)	0.5134(.059)	0.3536(.082)	0.2073(.181)
<b>TLVQM</b>	0.3988(.081)	0.5593(.195)	0.7170(.428)	0.5586(.096)	0.6165(.203)	0.7749(.432)	0.5923(.058)	0.3097(.096)	0.2578(.175)
<b>V-BLIINDS</b>	0.4042(.114)	0.4851(.235)	0.6833(.510)	0.6251(.123)	0.5316(.247)	0.7263(.506)	0.5502(.071)	0.4166(.096)	0.2428(.146)
<b>VIDEVAL</b>	0.3277(.124)	0.5438(.201)	0.7633(.418)	0.4521(.104)	0.6014(.202)	0.8109(.383)	0.6376(.054)	0.4047(.119)	0.2696(.210)
<b>ensemble</b>	0.6364(.063)	0.7211(.142)	0.8756(.271)	0.7979(.052)	0.7628(.152)	0.9168(.276)	0.4298(.052)	0.3020(.048)	0.1281(.107)
<b>ResNet50</b>	0.6006(.083)	0.7423(.126)	0.8370(.342)	0.7827(.059)	0.7868(.132)	0.9048(.295)	0.4420(.049)	0.2905(.043)	0.1362(.106)
<b>VGGFace</b>	0.5814(.111)	0.7673(.100)	0.9496(.144)	0.7710(.078)	0.7922(.113)	<b>0.9746(.056)</b>	0.4486(.054)	0.3049(.094)	0.1840(.189)
<b>DFDC-ispl</b>	0.5641(.092)	0.7582(.115)	0.8656(.275)	0.7868(.061)	0.8009(.129)	0.9407(.250)	0.4380(.047)	0.2825(.050)	0.1401(.097)
<b>DFGC-1st</b>	<b>0.7952(.051)</b>	<b>0.8081(.096)</b>	<b>0.9556(.129)</b>	<b>0.8975(.028)</b>	<b>0.8356(.106)</b>	0.9715(.082)	<b>0.3132(.030)</b>	<b>0.2540(.037)</b>	<b>0.1141(.105)</b>

average value over all testing iterations is reported to reflect model performances, and the standard deviation is also shown, which can imply the robustness of the models. As suggested in [24, 12], a nonlinear logistic function with four parameters is fitted to the predicted MOS before calculating the final metrics to improve prediction accuracy.

#### 4.2. Intra-subset Evaluation

**General Performance.** Table 4 shows a general image comparing different VRA models under our intra-subset evaluation protocols. As can be seen, the DFGC-1st model outperforms the others under nearly all metrics and protocols. The ensemble, VGG-Face, and DFDC-ispl models have the second-rank under some metrics and protocols. While the other hand-crafted IQA and VQA models suffer from obviously lower accuracy. The result of the DFGC-1st model leading the board implies that deepfake detection features may relate most to the VRA problem at hand. As an interesting comparison, one may wonder what is the correlation between the fake videos’ visual realism scores vs. their anti-detection scores. We use the detection scores output by the original DFGC-1st detection model subtracted from one as the anti-detection scores on all C3 videos. The result is SRCC=0.2651, and PLCC=0.3232, which indicates very little correlation. Since VRA and anti-detection scores originate from the same DFGC-1st features in this example, the result indicates that our feature selection and regression process play an important role in extracting VRA-related information.

**Table 5:** Comparison of video-level feature fusion strategies.

Metric	Fusion			PLCC↑	
	total	mean	std	id	submit-id
<b>ResNet50</b>	160	160	-	0.6787	0.7864
	220	-	220	0.7574	0.7635
	160	65	95	0.7827	0.7868
<b>DFGC-1st</b>	240	240	-	0.8711	0.8223
	280	-	280	0.8772	0.7949
	260	102	158	0.8975	0.8356

Comparing with the video level results, it is clear that the method level counterparts are much more accurate for all models and metrics. This shows that evaluating the realism performance for different face-swap methods are more tractable than that for individual videos. This result is not so unexpected, considering that method level evaluations can average out prediction noises on video instances.

**Comparison of video feature fusion strategies.** Table 5 shows the influence of adopting different video-level feature fusion strategies. The *Fusion* columns list the dimensions of selected features when using different fusion strategies, i.e., using both mean and std and using each pooling independently. It can be observed that using average pooling and standard deviation pooling together obviously boosts model performance. Features from  $f_{std}$  are selected more when using both fusion strategies, which implies the importance of standard deviation pooling for VRA models.

#### 4.3. Inter-subsets Evaluation

Table 6 demonstrates the results of prediction accuracy of models when trained and tested on different data subsets. Hand-crafted models are not tested here due to their high computational cost in feature extraction. The DFGC-1st model again surpasses the other models in terms of generalization ability. Although much better than a random guesser (random prediction in [1, 5]), all models have a clear performance degradation at video level compared to the intra-subset setting. The situation improves when coming to method level evaluations, but the accuracy gap between intra- and inter-subsets is still obvious. This calls for a further study on improving the generalization ability of VRA models. Note that for the test on the real videos, the mean prediction MOS should be close to 5 in ideal situations.

## 5. CONCLUSIONS

In this paper, we propose a benchmark for the new visual realism assessment (VRA) problem of face-swap videos. This benchmark is based on the DFGC-2022 dataset and includes several models from related fields which are used as feature

**Table 6:** Inter-subsets evaluation results

(a) Training on C3 and testing on C1							
model	SRCC↑		PLCC↑		RMSE↓		[8]
	video	method	video	method	video	method	
random	-0.0091		-0.0084		1.3727		
ResNet50	0.2384	0.4857	0.2978	0.7818	0.6834	0.3158	
VGG Face	0.2512	0.6571	0.2939	0.8315	0.6843	0.2813	
DFDC-ispl	0.3367	<b>0.9428</b>	0.3595	<b>0.9406</b>	0.6680	0.1719	
DFGC-1st	<b>0.3743</b>	0.6571	<b>0.4222</b>	0.7818	<b>0.6489</b>	<b>0.3158</b>	

(b) Training on C3 and testing on C2							
model	SRCC↑		PLCC↑		RMSE↓		[9]
	video	method	video	method	video	method	
random	0.0083		0.0083		1.411		
ResNet50	0.4173	0.6044	0.4027	0.7607	0.7460	0.4582	
VGG Face	0.4522	0.6813	0.4350	0.7580	0.7339	0.4605	
DFDC-ispl	0.3554	0.6978	0.3477	0.7698	0.7642	0.4507	
DFGC-1st	<b>0.5045</b>	<b>0.8846</b>	<b>0.4844</b>	<b>0.9088</b>	<b>0.7130</b>	<b>0.2946</b>	

(c) Training on C3 and testing on real videos			
model	mean pred MOS	std of pred MOS	RMSE↓
random	2.9967	1.1451	2.3084
ReNet50	3.7158	0.4409	1.3578
VGG Face	3.3768	0.3953	1.6707
DFDC-ispl	3.5502	0.3653	1.4951
DFGC-1st	<b>3.7685</b>	<b>0.2998</b>	<b>1.2675</b>

extractors. A SVR is trained as the regressor to predict realism scores for fake videos. We find that deep features beat most hand-crafted ones in this VRA task, with a deepfake detection model trained on diverse datasets, i.e., the DFGC-1st model, achieving the best performance, implying the close relation between deepfake realism assessment and its detection. However, improving VRA’s generalization ability under new datasets is still an open problem that requires further research. This work serves as a reference for future studies.

## 6. REFERENCES

- [1] Felix Juefei-Xu, Run Wang, Yihao Huang, Qing Guo, Lei Ma, and Yang Liu, “Countering malicious deepfakes: Survey, battleground, and horizon,” *International Journal of Computer Vision*, pp. 1–57, 2022.
- [2] Chen-Chou Lo, Szu-Wei Fu, Wen-Chin Huang, Xin Wang, Junichi Yamagishi, Yu Tsao, and Hsin-Min Wang, “MOSNet: Deep Learning-Based Objective Assessment for Voice Conversion,” in *Proc. Interspeech 2019*, 2019, pp. 1541–1545.
- [3] Ryandhimas E. Zezario, Szu-Wei Fu, Fei Chen, Chiou-Shann Fuh, Hsin-Min Wang, and Yu Tsao, “Deep learning-based non-intrusive multi-objective speech assessment model with cross-domain features,” *IEEE/ACM Transactions on Audio, Speech, and Language Processing*, vol. 31, pp. 54–70, 2023.
- [4] Sophie J Nightingale and Hany Farid, “Ai-synthesized faces are indistinguishable from real faces and more trustworthy,” *Proceedings of the National Academy of Sciences*, vol. 119, no. 8, pp. e2120481119, 2022.
- [5] Sophie Nightingale, Shruti Agarwal, Erik Härkönen, Jaakko Lehtinen, and Hany Farid, “Synthetic faces: how perceptually convincing are they?,” *Journal of Vision*, vol. 21, no. 9, pp. 2015–2015, 2021.
- [6] Pavel Korshunov and Sébastien Marcel, “Deepfake detection: humans vs. machines,” *arXiv preprint arXiv:2009.03155*, 2020.
- [7] Yu Tian, Zhangkai Ni, Baoliang Chen, Shiqi Wang, Hanli Wang, and Sam Kwong, “Generalized visual quality assessment of gan-generated face images,” *arXiv preprint arXiv:2201.11975*, 2022.
- [8] Bo Peng, Wei Xiang, Yue Jiang, Wei Wang, Jing Dong, Zhenan Sun, Zhen Lei, and Siwei Lyu, “Dfgc 2022: The second deepfake game competition,” in *2022 IEEE International Joint Conference on Biometrics (IJB)*, 2022, pp. 1–10.
- [9] Ivan Perov, Daiheng Gao, Nikolay Chervoniy, Kunlin Liu, Sugasa Marangonda, Chris Umé, Mr Dpfks, Carl Shift Facenheim, Luis RP, Jian Jiang, et al., “Deepfacelab: Integrated, flexible and extensible face-swapping framework,” *arXiv preprint arXiv:2005.05535*, 2020.
- [10] Renwang Chen, Xuanhong Chen, Bingbing Ni, and Yanhao Ge, “Simswap: An efficient framework for high fidelity face swapping,” in *Proceedings of the 28th ACM International Conference on Multimedia*, 2020, pp. 2003–2011.
- [11] Lingzhi Li, Jianmin Bao, Hao Yang, Dong Chen, and Fang Wen, “Advancing high fidelity identity swapping for forgery detection,” in *Proceedings of the IEEE/CVF Conference on Computer Vision and Pattern Recognition*, 2020, pp. 5074–5083.
- [12] Zhengzhong Tu, Yilin Wang, Neil Birkbeck, Balu Adsumilli, and Alan C Bovik, “Ugc-vqa: Benchmarking blind video quality assessment for user generated content,” *IEEE Transactions on Image Processing*, vol. 30, pp. 4449–4464, 2021.
- [13] Anish Mittal, Anush Krishna Moorthy, and Alan Conrad Bovik, “No-reference image quality assessment in the spatial domain,” *IEEE Transactions on Image Processing*, vol. 21, no. 12, pp. 4695–4708, 2012.
- [14] Deepti Ghadiyaram and Alan C Bovik, “Perceptual quality prediction on authentically distorted images using a bag of features approach,” *Journal of Vision*, vol. 17, no. 1, pp. 32–32, 2017.
- [15] Wufeng Xue, Xuanqin Mou, Lei Zhang, Alan C Bovik, and Xiangchu Feng, “Blind image quality assessment using joint statistics of gradient magnitude and laplacian features,” *IEEE Transactions on Image Processing*, vol. 23, no. 11, pp. 4850–4862, 2014.
- [16] Jari Korhonen, “Two-level approach for no-reference consumer video quality assessment,” *IEEE Transactions on Image Processing*, vol. 28, no. 12, pp. 5923–5938, 2019.
- [17] Michele A Saad, Alan C Bovik, and Christophe Charrier, “Blind prediction of natural video quality,” *IEEE Transactions on Image Processing*, vol. 23, no. 3, pp. 1352–1365, 2014.
- [18] Zhengzhong Tu, Xiangyu Yu, Yilin Wang, Neil Birkbeck, Balu Adsumilli, and Alan C Bovik, “Rapique: Rapid and accurate video quality prediction of user generated content,” *IEEE Open Journal of Signal Processing*, vol. 2, pp. 425–440, 2021.
- [19] Karen Simonyan and Andrew Zisserman, “Very deep convolutional networks for large-scale image recognition,” in *Proceedings of the 3rd International Conference on Learning Representations*, 2015.
- [20] Kaiming He, Xiangyu Zhang, Shaoqing Ren, and Jian Sun, “Deep residual learning for image recognition,” in *Proceedings of the IEEE conference on computer vision and pattern recognition*, 2016, pp. 770–778.
- [21] O Parkhi, A Vedaldi, and A Zisserman, “Deep face recognition,” in *Proceedings of the British Machine Vision Conference*, 2015, pp. 1–12.
- [22] “DFGC-2022 first-place solution of the detection track,” <https://github.com/chenhanch/DFGC-2022-1st-place>.
- [23] Nicolò Bonettini, Edoardo Daniele Cannas, Sara Mandelli, Luca Bondi, Paolo Bestagini, and Stefano Tubaro, “Video face manipulation detection through ensemble of cnns,” in *2020 25th International Conference on Pattern Recognition (ICPR)*. IEEE, 2021, pp. 5012–5019.
- [24] Kalpana Seshadrinathan, Rajiv Soundararajan, Alan Conrad Bovik, and Lawrence K Cormack, “Study of subjective and objective quality assessment of video,” *IEEE transactions on Image Processing*, vol. 19, no. 6, pp. 1427–1441, 2010.